Vol. 13(17), pp. 243-249, 30 October, 2018
DOI: 10.5897/IJPS2018.4750
Article Number: DF4FB0C59119
ISSN: 1992-1950

http://www.academicjournals.org/IJPS

ACADEMIC JOURNALS
expand your knowledge

International Journal of Physical Sciences

Full Length Research Paper

Deriving an expression for electron-reflection-coefficient at metal-semiconductor-interface of dye-sensitized solar cells

Lurwan Garba

Department of Physics, Faculty of Science, Northwest University, 3220 Kano, Nigeria.

Received 9 July, 2018; Accepted 16 September, 2018

This work aims to derive an expression to describe the reflection coefficient of an escape electron from metal-semiconductor interface of DSSC. The derivation was obtained by analytically solving electron diffusion equation with assumptions of steady state DSSC and negligible current flow at the outer most part of the film. The derived corrected Richardson-Dushman equation including a reflection of electron wave at potential barrier is inserted into current-voltage (JV) characteristic equation. We showed that voltage loss at various temperature and current densities do not vary with and without reflection coefficient. However, the reflection coefficient is shown to be insignificant to JV characteristics with respect to potential barriers. Our results confirm the effect of potential barrier through which an electron must be accelerated in order to gain sufficient energy necessary for high power conversion efficiency.

Key words: DSSC, drift-diffusion, metal-semiconductor, reflection coefficient.

INTRODUCTION

Development of clean energy represents one of the society's foremost challenges in 21st century. Modern civilization and developments in all aspects have been rapidly accelerating with increase in energy demand and consumption which serve as characteristics for civilizations (Li and Wu, 2015). The non-renewable sources of energy are inevitably disappearing leaving renewable sources like the sun. Sunlight is a compelling solution to our need for clean and abundant energy sources, with potential capacity to supply world's current energy demands. The sun supplied about $95 \times 10^{15} J/s$ amount of energy to the Earth surface which is ten thousand times greater than our todays' energy needs (Grätzel, 2005). Surprisingly, solar energy today accounts for <2% of world's energy use. Reducing this huge gap requires both theoretical and experimental research in the development of technology for high performance and low cost solar cells. Consequently, solar cells have increasingly received attentions over the last decades. With achievement in Dye- Sensitized Solar cells (DSSC)

E-mail: ridwangy@yahoo.com.

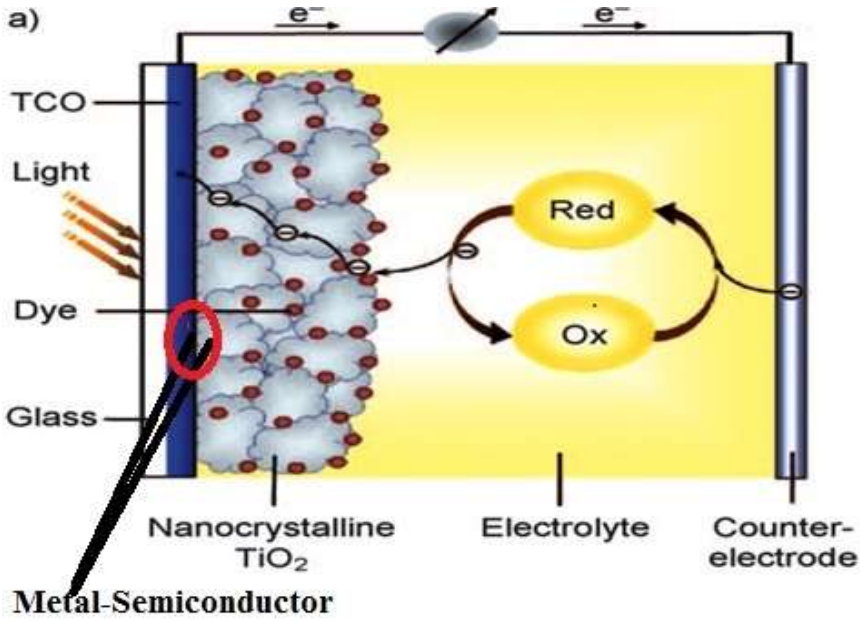

Figure 1. Scheme of a Dye-Sensitized Solar Cell (DSSC).

energy conversion efficiency to about 14% (Dong et al., 2015; Pan et al., 2014), the DSSC technology has attracted much attention for developing low-cost, high-efficiency solar energy conversion (Dai et al., 2005; Hagfeldt et al., 1994; Knödler et al., 1993; Ni et al., 2006; O'regan and Grfitzeli, 1991; Pettersson and Gruszecki, 2001; Smestad, 1994). DSSC is one type of Photo-electrochemical solar cells also called photovoltaic cells belonging to thin film group solar cell which is designed to convert solar radiation directly into electricity. The first version of a dye solar cell was developed by O'Rangen and Gratzel in 1991 (O'Regan et al., 2000; O'regan and Grfitzeli, 1991). It is based on semiconductor formed between a photo-sensitized anode and an electrolyte. It reported high efficiency based on titanium oxide (TiO_2) nanoparticles and transparent conducting glass (TCO). However, there are many other solar energy conversion techniques; such as photo-galvanic cells which have been investigated for conversion and storage of low intensity solar energy under artificial sunlight (Calogero et al., 2015; Gangotri and Koli, 2017; Koli, 2017).

MATERIALS AND METHODS

Figure 1 shows the diagram of a typical DSSC. It mainly composes of a transparent conductive oxide (TCO), an electron acceptor in form of a wide band-gap semiconductor, a light-absorbing molecular dye, a liquid or solid redox solution forming a conducting medium and a platinum-coated TCO as cathode. The TiO_2 (serving as wide band-gap semiconductor) together with TCO and molecular dye forms the photo-anode of the cell. The medium of conduction is sandwiched between photo-anode and platinum-based cathode. The most typically used mediators are I_3^-/I^- redox couple in a liquid electrolyte (Samanchandra et al., 2017; Sawhney et al., 2017). The red circle shows the interface between TCO-metal and TiO_2-semiconductor.

The photo-electrode is sensitized to visible light by adsorbing a molecular dye (Akın et al., 2016; Lim et al., 2014). When photon is absorbed, the dye gets excited which leads to injection of electrons into metal oxide substrate. This injected electrons will then move through nano-crystalline TiO_2 to TCO and then flows directly to counter electrode via external circuit (Mao et al., 2016). The oxidized dye molecules are regenerated by redox mediators I_3^-/I^- (Bonomo et al., 2016). Lastly, the oxidized redox mediators I_3^-/I^- are transported to counter electrode for further regeneration to occur and to complete the DSSC operational cycle (Govindaraj et al., 2014; Imoto et al., 2003; Papageorgiou et al., 1996; Wei et al., 2014). Efficient electron injection coming from the excited dye to the nano-crystalline TiO_2 plays a great role in the DSSC performance (Cavallo et al., 2017; Cherepy et al., 1997; Franco et al., 1999) and these electrons are mainly transported through diffusion (Anta et al., 2006; Bisquert et al., 2004). In theory, it is assumed that induced photo-voltage is equal to the difference between quasi-Fermi level (E_F) of TiO_2 and electrolyte redox potential (R_{edox}) (Ferber et al., 1998; Gómez and Salvador, 2005; Soedergren et al., 1994). This work derived the significance of reflection coefficient to current-voltage (JV) characteristics with respect to potential barriers.

DERIVATIONS

Voltage between TiO_2, Fermi level (E_f) and the redox potential of electrolyte

The expression for action spectra and current-voltage behavior for substrate/electrode interface can be made

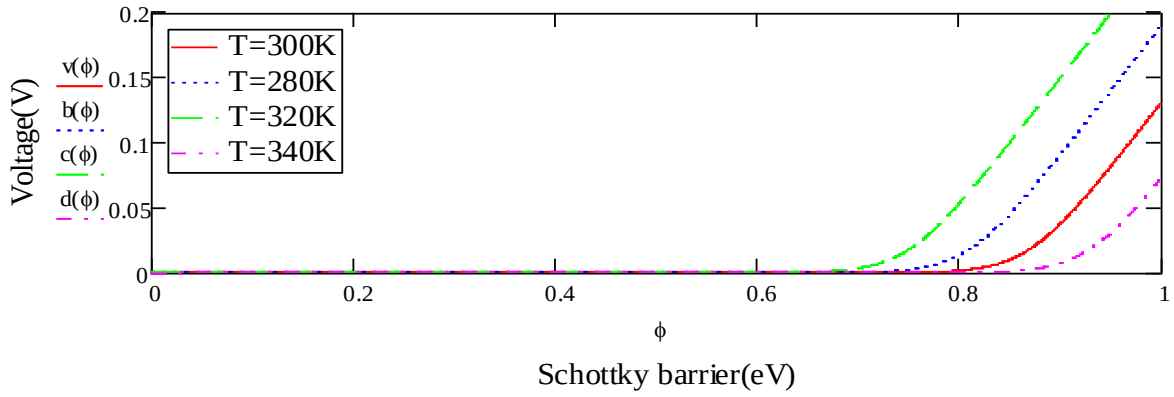

Figure 2. Voltage loss at TiO_2/TCO with Schotty barrier and temperature.

by considering 3-dimensional isotropic micro-porous network consisting of nano-sized low-doped semiconducting colloids (Cavallo et al., 2017; Soedergren et al., 1994). The electrolyte is able to penetrate the film all way to back contact, and every colloid will be in contact with the electrolyte (Kuzmych, 2014). This will deplete all charge carriers, and there will be no band bending. The charge concentration in valence and conduction bands in dark is then totally determined by choice of redox couple. The derivation will be made for electrons as charge carriers in the film, and electron current taken to be positive. Two assumptions were made; the transport of electrons in semiconductor takes place through diffusion and that electron diffusion length is constant through TiO_2 film, such that recombination process takes over. Therefore, the current-voltage characteristic is derived from diffusion equation for electrons in TiO_2 thin film. The continuity diffusion equation that described the transport, recombination and generation of electrons within the nanoporous film is given by;

$$D\frac{\partial^2 n(x)}{\partial x^2} - \frac{1}{\tau}[n(x) - n_0] + \Phi\alpha e^{(-\alpha x)} = \frac{\partial n}{\partial t} \quad (1)$$

Where, $n(x)$ is excess density of electrons at an x position within the film from (TCO/ TiO_2) interface, n_0 is electron density in dark condition, D is electron diffusion coefficient, τ is mean electron lifetime, Φ and α are incident photon intensity and photon absorption coefficient respectively. In a steady state condition of an irradiated DSSC, this equation becomes;

$$D\frac{\partial^2 n(x)}{\partial x^2} - \frac{1}{\tau}[n(x) - n_0] + \Phi\alpha e^{(-\alpha x)} = 0 \quad (2)$$

When the circuit is unloaded (short-circuit condition) $x = 0$, electrons are drawn off as a photocurrent and none of electrons are extracted directly to counter electrode, therefore, the boundary condition is: $n(0) = n_0$. Similarly, electrons reaching outer most part of TiO_2 film ($x = d$), are reflected and diffused back again into inner layer of the film, hence, there is a negligible current flow at $x = d$, (d is film thickness); then we have the second boundary condition; $\frac{dn(x)}{dx}_{x=d} = 0$. Using condition these two conditions, we can solve equation (2) to get short-circuit current as given by;

$$I_{sc} = \frac{q\Phi}{1 - L^2\alpha^2} L\alpha \left[\frac{L\alpha e^{(-d\alpha)}}{cosh\left(\frac{d}{L}\right)} + tanh\left(\frac{d}{L}\right) - L\alpha\right] \quad (3)$$

Where, $L = \sqrt{D\tau}$ is electron diffusion length, q is charge of an electron. Operating the DSSC by varying external potential difference V and recording current between Fermi level of TiO_2 and electrolyte redox potential which resulted from photo-irradiation, the density of electrons at TCO/TiO_2 interface increases to n, and this gives a new boundary condition: $n(0) = n$. While for $x = d$, electrons at outer most part of the film are still reflected and diffuse back into inner layer of the film, and therefore no/negligible current flow is recoded. However, this change in potential due to excess density of photo-generated electrons at back contact/semiconductor interface give rise to photo-voltage given as;

$$V_0 = \frac{1}{q} kTm \left[ln\frac{n_{contact}}{n_0}\right] \quad (4)$$

Where, T is absolute temperature, k is Boltzmann's constant and m is an ideality factor which is equal to 2 (Cameron and Peter, 2005) (Figure 2).

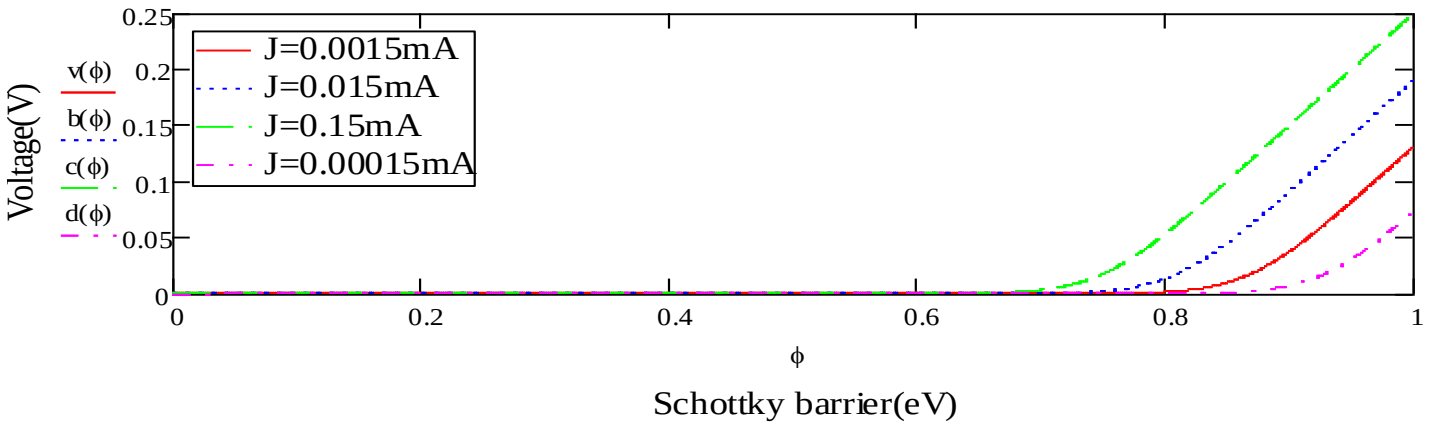

Figure 3. Voltage loss at TiO_2/TCO with Schotty barrier and current density.

Therefore, solving the steady-state diffusion equation using these boundary conditions and through use of equation (4), we get current-voltage relations as;

$$I = I_{sc} - \frac{qDn_0}{L} tanh\left(\frac{d}{L}\right)\left[exp\left(qV_0/kTm\right) - 1\right] \quad (5)$$

However, for an optimal solar cell, diffusion length is larger than film thickness (i.e. $L > d$), then Equation (5) becomes;

$$I = I_{sc} - \frac{qn_0 d}{\tau}\left[exp\left(qV_0/kTm\right) - 1\right. \quad (6)$$

Where, $\tau = \frac{L^2}{D}$ and is determined by recombination kinetics at Semiconductor/Electrolyte Interface (SEI). Generally, ignoring the area of the DSSC from equation (5), the current-voltage characteristic can be given as;

$$I = I_{sc} - I_{sa}\left[exp\left(qV/kTm\right) - 1\right] \quad (7)$$

Where, I_{sa} is saturation current and is always constant for a given solar cell.

Thermionic emission: Metal-semiconductor (TCO/TiO_2) interface

In his model, Meng et al. (Ni et al., 2006) considered TCO substrate as a metal which is highly doped with high electrical conductivity and simulates the TCO/TiO_2 interface by Schottky barrier model (Figure 3). Under photo-incident on the cell, electron flow through TCO/TiO_2 interface causes loss of voltage which can be given from thermionic emission theory as;

$$V_1 = \frac{kT}{q} ln\left[\frac{I}{I_{sa}} + 1\right] \quad (8)$$

Where, I_{sa} is saturation current.

Saturation current

The electron in metal requires a minimum amount of energy for its emission from metal surface either by photo-electric process or by heating of the metal. This minimum energy E_0 is called work function of the metal. If q is charge of an electron and ϕ_0 is potential difference through which an electron must be accelerated in order to gain an energyE_0, then, $E_0 = q\phi_0$. According to free electron theory of metals, electrons are free to move about inside a metal; however, they cannot normally come out of the metal surface because they are in an attractive electric field due to positive ions at lattice sites of the metals. The positive ions will generate within the metal, a positive potential field which varies periodically from point to point. The free electron model can be used to deduce Richardson-Dushman equation for variation of saturation electron current density evaporated from a heated metallic body, to be given by:

$$I_{sa} = AT^2 e^{\left(-q\phi_0/kT\right)} \quad (9)$$

Where, A is a constant given by:

$$A = \frac{mqk^2}{2\pi^2\hbar^3} \quad (10)$$

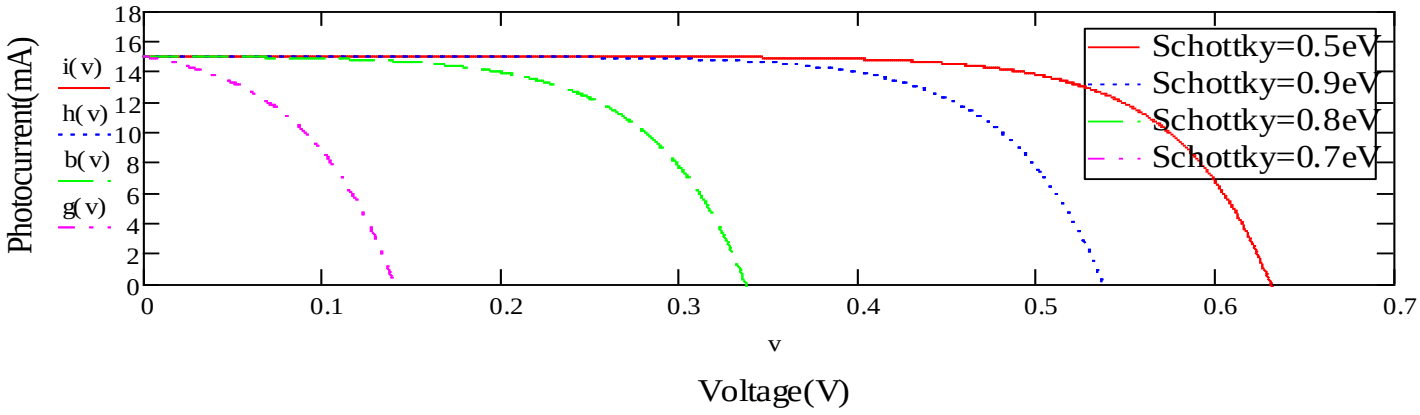

Figure 4. Effect of TiO_2/TCO Schotty barrier height on DSSCJ-V characteristics.

m is free electron mass, and $\hbar = \frac{h}{2\pi}$, h is Planck's constant.

Combining Equations (9) and (7) we get voltage loss to be;

$$V_1 = \frac{kT}{q} ln\left[\frac{I}{AT^2 e^{\left(-q\phi_0/kT\right)}} + 1\right] \tag{11}$$

Equation (9) is Richardson-Dushman equation which does not take into consideration reflection of electron wave at the potential barrier that must be crossed by electrons at the time of emission from the metal surface. This is a quantum mechanical effect and can be taken into account by introducing a quantum mechanical reflection coefficient $R(v_x)$ which depends on x component of the electron velocity v_x (Figure 4).

Effect of reflection coefficient on saturation current

In other for electron to be emitted from the metal, it must overcome the attractive force acting at a right angle to the metal surface. If the metal surface coincides with y-z plane, then the force will act along x-direction and therefore, x-component of the electron velocity must be such that kinetic energy $(\frac{mv_x{}^2}{2})$ exceeds the minimum energy E_0 needed for emission of the electron. The components of electron velocities $v_y \; and \; v_z$ may extend from negative infinity to positive infinity. The number of such electrons with x-component of velocity lying in the interval $v_x \; to \; v_x + dv_x$ is

$$n(v_x)dv_x = \frac{1}{4}\left(\frac{m}{\pi\hbar}\right)^3 exp\left(\frac{E_f}{kT}\right) exp\left(\frac{-mv_x{}^2}{2kT}\right) dv_x * \int_{-\infty}^{+\infty} exp\left(\frac{-mv_y{}^2}{2kT}\right) dv_y * \int_{-\infty}^{+\infty} exp\left(\frac{-mv_z{}^2}{2kT}\right) dv_z \tag{12}$$

The values of the two integrals on RHS are well known to be;

$$\int_{-\infty}^{+\infty} exp\left(\frac{-mv_y{}^2}{2kT}\right) dv_y = \int_{-\infty}^{+\infty} exp\left(\frac{-mv_z{}^2}{2kT}\right) dv_z = \sqrt{\frac{2\pi kT}{m}} \tag{13}$$

Therefore, we get;

$$n(v_x)dv_x = \frac{kT}{2\hbar^3}\left(\frac{m}{\pi}\right)^2 exp\left(\frac{E_f}{kT}\right) exp\left(\frac{-mv_x{}^2}{2kT}\right) dv_x$$

And the number of electrons crossing a unit area per second in x-direction with $v_x > v_0$ is

$$n = \int_{v_0}^{\infty} v_x n(v_x)dv_x = \frac{kT}{2\hbar^3}\left(\frac{m}{\pi}\right)^2 exp\left(\frac{E_f}{kT}\right) \int_{v_0}^{\infty} v_x exp\left(\frac{-mv_x{}^2}{2kT}\right) dv_x \tag{14}$$

Where, $v_0 = \sqrt{\frac{2E_0}{m}}$.

However, incorporating this equation with reflection coefficient, we get,

$$n = \frac{kT}{2\hbar^3}\left(\frac{m}{\pi}\right)^2 exp\left(\frac{E_f}{kT}\right) \int_{v_0}^{\infty} v_x exp\left(\frac{-mv_x{}^2}{2kT}\right) \left(1 - R(v_x)\right) dv_x \tag{15}$$

Assuming that reflection coefficient does not vary appreciably over small velocity range for which major contribution to the integral in above equation comes, then we can take an average value of reflection coefficient and take the factor $\left(1 - R(v_x)\right)$ outside the integral sign, such that the saturation current takes the form;

$$I_s = AT^2\left(1 - R(v_x)\right) exp\left(-q\phi_0/kT\right) \tag{16}$$

This is the Richardson-Dushman equation corrected for reflection of electron wave at the potential barrier. Therefore,

$$ln\left(\frac{I_s}{T^2}\right) = ln[A(1-R)] - \frac{q\phi_0}{kT} \quad (17)$$

A straight line with slope equals to $-\frac{q\phi_0}{T}$ and intercept is $ln[A(1-R)]$ when $ln\left(\frac{I_s}{T^2}\right)$ is plotted against $\left(\frac{1}{kT}\right)$

Conclusion

In this work, we derived saturation current equation corrected to include effect of electron reflection coefficient in metal-semiconductor interface of a DSSC. Our results showed less significant impact of reflection coefficient at barrier potential of the DSSC to current-voltage characteristics which further confirms the effect of this potential in accelerating emitted electrons to attain high energy that is needed for high conversion efficiency. We showed effects of barrier potential in accelerating electrons which attain adequate energy that is needed for efficient high power conversion.

CONFLICT OF INTERESTS

The author has not declared any conflict of interest.

ACKNOWLEDGEMENTS

The authors are indebted to Prof. Dr. Abdul Kariem Bin Mohd Arof of the Department of Physics, University of Malaya for his inspirational talks on this field of research. We are equally grateful to Northwest University Kano, Nigeria.

REFERENCES

Akın S, Gülen M, Sayın S, Azak H, Yıldız HB, Sönmezoğlu S (2016). Modification of photoelectrode with thiol-functionalized Calix [4] arenes as interface energy barrier for high efficiency in dye-sensitized solar cells. Journal of Power Sources 307:796-805.

Anta JA, Casanueva F, Oskam G (2006). A numerical model for charge transport and recombination in dye-sensitized solar cells. The Journal of Physical Chemistry B 110(11):5372-5378.

Bisquert J, Cahen D, Hodes G, Rühle S, Zaban A (2004). Physical chemical principles of photovoltaic conversion with nanoparticulate, mesoporous dye-sensitized solar cells. The Journal of Physical Chemistry B 108(24):8106-8118.

Bonomo M, Dini D, & Marrani AG (2016). Adsorption Behavior of I3–and I–Ions at a Nanoporous NiO/Acetonitrile Interface Studied by X-ray Photoelectron Spectroscopy. Langmuir 32(44):11540-11550.

Calogero G, Bartolotta A, Di Marco G, Di Carlo A, Bonaccorso F (2015). Vegetable-based dye-sensitized solar cells. Chemical Society Reviews 44(10):3244-3294.

Cameron PJ, Peter LM (2005). How does back-reaction at the conducting glass substrate influence the dynamic photovoltage response of nanocrystalline dye-sensitized solar cells? The Journal of Physical Chemistry B, 109(15):7392-7398.

Cavallo C, Di Pascasio F, Latini A, Bonomo M, Dini D (2017). Nanostructured semiconductor materials for dye-sensitized solar cells. Journal of Nanomaterials.

Cherepy NJ, Smestad GP, Grätzel M, Zhang JZ (1997). Ultrafast electron injection: implications for a photoelectrochemical cell utilizing an anthocyanin dye-sensitized TiO2 nanocrystalline electrode. The Journal of Physical Chemistry B 101(45):9342-9351.

Dai S, Wang K, Weng J, Sui Y, Huang Y, Xiao S, Pan X (2005). Design of DSC panel with efficiency more than 6%. Solar Energy Materials and Solar Cells 85(3):447-455.

Dong H, Wu Z, El-Shafei A, Xia B, Xi J, Ning S, Hou X (2015). Ag-encapsulated Au plasmonic nanorods for enhanced dye-sensitized solar cell performance. Journal of Materials Chemistry A 3(8):4659-4668.

Ferber J, Stangl R, Luther J (1998). An electrical model of the dye-sensitized solar cell. Solar Energy Materials and Solar Cells 53(12):29-54.

Franco G, Gehring J, Peter L, Ponomarev E, Uhlendorf I (1999). Frequency-resolved optical detection of photoinjected electrons in dye-sensitized nanocrystalline photovoltaic cells. The Journal of Physical Chemistry B 103(4):692-698.

Gangotri P, Koli P (2017). Study of the enhancement on photogalvanics: solar energy conversion and storage in EDTA–safranine O–NaLS system. Sustainable Energy and Fuels 1(4):882-890.

Gómez R, Salvador P (2005). Photovoltage dependence on film thickness and type of illumination in nanoporous thin film electrodes according to a simple diffusion model. Solar Energy Materials and Solar Cells 88(4):377-388.

Govindaraj R, Pandian MS, Ramasamy P, Mukhopadhyay S (2014). Synthesis of titanium dioxide nanostructures and their effects on current-voltage (IV) performance in dye sensitized solar cells. International Journal Chemical Technology Research 6(13):5220-5225.

Grätzel M (2005). Solar energy conversion by dye-sensitized photovoltaic cells. Inorganic chemistry 44(20):6841-6851.

Hagfeldt A, Didriksson B, Palmqvist T, Lindström H, Södergren S, Rensmo H, Lindquist SE (1994). Verification of high efficiencies for the Grätzel-cell. A 7% efficient solar cell based on dye-sensitized colloidal TiO 2 films. Solar Energy Materials and Solar Cells 31(4):481-488.

Imoto K, Takahashi K, Yamaguchi T, Komura T, Nakamura J, Murata K (2003). High-performance carbon counter electrode for dye-sensitized solar cells. Solar Energy Materials and Solar Cells 79(4):459-469.

Knödler R, Sopka J, Harbach F, Grünling H (1993). Photoelectrochemical cells based on dye sensitized colloidal TiO2 layers. Solar energy materials and solar cells 30(3):277-281.

Koli P (2017). Surfactant and natural sunlight enhanced Photogalvanic effect of Sudan I dye. Arabian Journal of Chemistry 10(8):1077-1083

Kuzmych O (2014). Development and characterization of dye-and semiconductor sensitized solar cells based on structurally organized titanium dioxide. (PhD), University of Warsaw.

Li J, Wu N (2015). Semiconductor-based photocatalysts and photoelectrochemical cells for solar fuel generation: a review. Catalysis Science and Technology 5(3):1360-1384.

Lim SP, Pandikumar A, Huang NM, Lim HN (2014). Enhanced photovoltaic performance of silver@ titania plasmonic photoanode in dye-sensitized solar cells. RSC Advances 4(72):38111-38118.

Mao X, Zhou R, Zhang S, Ding L, Wan L, Qin S, Miao S (2016). High efficiency dye-sensitized solar cells constructed with composites of TiO 2 and the hot-bubbling synthesized ultra-small SnO 2 nanocrystals. Scientific Reports 6:19390.

Ni M, Leung MK, Leung DY, Sumathy K (2006). Theoretical modeling of TiO 2/TCO interfacial effect on dye-sensitized solar cell performance. Solar energy materials and solar cells, 90(13):2000-2009.

O'Regan B, Schwartz DT, Zakeeruddin SM, Grätzel M (2000). Electrodeposited Nanocomposite n–p Heterojunctions for Solid-State Dye-Sensitized Photovoltaics. Advanced Materials 12(17):1263-1267

O'regan B, Grfitzeli M (1991). A low-cost, high-efficiency solar cell based on dye-sensitized. Nature 353(6346):737-740.

Pan Z, Mora-Seró I, Shen Q, Zhang H, Li Y, Zhao K, Bisquert J (2014). High-efficiency "green" quantum dot solar cells. Journal of the American Chemical Society 136(25):9203-9210.

Papageorgiou N, Grätzel M, Infelta P (1996). On the relevance of mass transport in thin layer nanocrystalline photoelectrochemical solar cells. Solar Energy Materials and Solar Cells 44(4):405-438.

Pettersson H, Gruszecki T (2001). Long-term stability of low-power dye-sensitised solar cells prepared by industrial methods. Solar Energy Materials and Solar Cells 70(2):203-212.

Samanchandra AR, Tharanga D, Sewvandi GA (2017). Fabrication of dye sensitized solar cells using locally available sensitizers. Paper presented at the Engineering Research Conference (MERCon), 2017 Moratuwa.

Sawhney N, Raghav A, Satapathi S (2017). Utilization of naturally occurring dyes as sensitizers in dye sensitized solar cells. IEEE Journal of Photovoltaics 7(2):539-544.

Smestad G (1994). Testing of dye sensitized TiO 2 solar cells II: Theoretical voltage output and photoluminescence efficiencies. Solar energy materials and solar cells 32(3):273-288.

Soedergren S, Hagfeld A, Olsson J, Lindquist SE (1994). Theoretical models for the action spectrum and the current-voltage characteristics of microporous semiconductor films in photoelectro-chemical cells. The Journal of Physical Chemistry 98(21):5552-5556.

Wei M, Fan Z, Sheng M (2014). Dye-sensitized solar cells: Atomic scale investigation of interface structure and dynamics. Chinese Physics B *23*(8):086801.